Saint-Venant torsion of functional graded orthotropic piezoelectric hollow circular cylinder

ISTVÁN ECSEDI, ATTILA BAKSA
Institute of Applied Mechanics
University of Miskolc
H-3515 Miskolc-Egyetemváros, Miskolc
HUNGARY

Abstract: This paper gives an analytical solution to the Saint-Venant torsion of the hollow and solid circular cylinder made of orthotropic functionally graded piezoelectric material. The elastic flexibility coefficients and piezoelectric constants and permittivities have only radial dependence. The considered material non-homogeneity is described by power function. The solution of the Saint-Venant torsion problem is presented for Prandtl's stress function, shearing stresses, electric displacement potential function, torsion function and electric potential function. An example illustrates the application of the formulated analytical method.

Key-Words: Saint-Venant torsion, piezoelectricity, Prandtl's stress function, functionally graded, radial non-homogeneity

Received: August 28, 2022. Revised: February 21, 2023. Accepted: March 20, 2023. Published: April 20, 2023.

1 Introduction

Examining the relationship between mechanical deformations and elastic fields is a very important task. Study by Altzoumailis and Kytopoulos deals with the connection of applied elastic stress to the micromagnetic activity of steels [1]. It is shown that an increase in supplied elastic strain leads to the broadening of both distribution modes. The following essential conclusion can be done in [1]: elastic stress applied far from below the macroscopic elastic limit, may facilitate suitable quantitative as well as qualitative changes in the micromagnetic activity of ferromagnetic steels. Paper [2] describes a fully integrated acoustic sensor that combines high sensitivity in wide frequency range. The Saint-Venant torsion of a homogenous, isotropic elastic cylindrical body is a classical problem of elasticity [3,4,5], which is solved using a semi inverse method by assuming a state of pure shear in the cylindrical body so that it gives rise to a resultant torque over the end cross sections. Extension of more complicated cases of anisotropic or non-homogeneous materials has been considered by Lekhnitskii [6,7], Rooney and Ferrai [8], Davi [9], Bisegna [10,11], Horgan and Chan [12], Rovenski et. al. [13,14], Rovenski and Abramovich [15], Horgan [16], Ecsedi and Baksa [17,18,19].

In this paper, the torsional deformation of radially non-homogeneous piezoelectric solid and hollow circular cylinders is studied. The material of the circular cylinder is functionally graded. In the considered case the dependence of the material parameters from the radial coordinate is described by a smooth function of the radial coordinate [21,22]. In the present problem the power law distribution is prescribed. Let K be an arbitrary material parameter its dependence of the radial coordinate is given by equation (1)

$$K(r) = f(r)k, \qquad (1)$$

where

$$f(r) = f_1\left(\frac{r-R_2}{R_1-R_2}\right)^n + f_2\left(\frac{r-R_1}{R_2-R_1}\right)^n$$

$$f_1 > 0 \;\; f_2 > 0 \;\; f_1 + f_2 = 1. \qquad (2)$$

In equation (2) R_1 and R_2 are the radii of the inner and outer boundary circle of the cross section A (see Figure 1), f_1, f_2 and n are material parameter. f_1 and f_2 are units free.

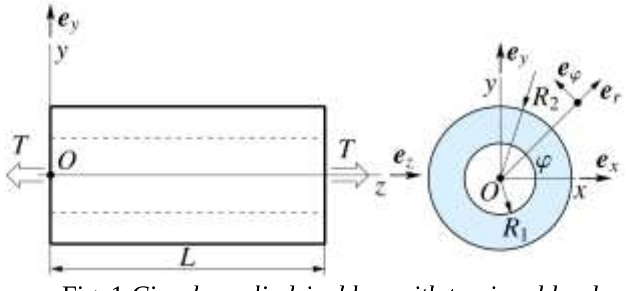

Fig. 1 *Circular cylindrical bar with torsional load*.

The applied torque is denoted by T and the unit vectors of the Cartesian coordinate system $Oxyz$ are $\boldsymbol{e}_x$, $\boldsymbol{e}_y$ and $\boldsymbol{e}_z$ (see Figure 1). Later on the polar coordinates r, φ, z will be used which are defined as

$$r = \sqrt{x^2 + y^2} \quad \varphi = \arctan\frac{y}{x}. \tag{3}$$

The unit vectors of the polar coordinate system $Or\varphi z$ are $\boldsymbol{e}_r$, $\boldsymbol{e}_\varphi$ and $\boldsymbol{e}_z$ (see Fig. 1).

The formulation of the Saint-Venant's theory of uniform torsion for homogenous piezoelectric beams has been given by Dave [9], Bisegna [10,11] and Rovenski et al. [13,14]. The papers of Bisegna [10,11] use the Prandtl's stress function and electric displacement potential function for simply connected cross section. Davi [9] obtained a coupled boundary-value problem for the torsion function and for the electric potential function from a constrained three dimensional static problem by the application of the usual assumptions of the Saint-Venant's theory. Rovenski et al. [13,14] give a torsion and electric potential functions formulation of the Saint-Venant's torsion problem for monoclinic homogeneous piezoelectric beams. In these papers [13,14], a coupled Neumann problem is derived for the torsion and electric potential functions, where exact and numerical solutions for elliptical and rectangular cross sections are presented. Ecsedi and Baksa give a formulation of the Saint-Venant torsion for homogeneous monoclinic piezoelectric beams in terms of Prandt's stress function and electric displacement potential function. The Prandtl's stress function and electric displacement potential function satisfy a coupled Dirichlet problem in the multiply connected cross section. A direct formulation and a variational formulation are developed in paper [17]. In an another paper by Ecsedi and Baksa [18], a variational formulation of the uniform torsion is presented for homogeneous linear piezoelectric monoclinic beams. The variational formulation uses the torsion and electric potential functions as independent quantities in paper [18]. Rovenski and Abramovich apply a linear analysis to piezoelectric beams with non-homogeneous cross sections that consist of various monoclinic piezoelectric and elastic materials [15]. They give the solution procedure for extension, bending, torsion and shearing. The developed theoretical method is illustrated by numerical examples [15]. Paper [20] deals with radially non-homogenous orthotropic piezoelectric circular cylinder, where the fundamental variables are the torsion function and electric potential function, so called c^E_{ijkl}, e_{kij}, ε^s_{ik} formulation is used.

2 Governing equations

Let $B = A \times (0, L)$ be a right circular cylinder. Let A_1 and A_2 be the bases of the cylinder and let $A_3 = \partial A \times (0, L)$ the mantle of the cylinder B (see Figure 1). The cross section of the cylinder is A and its boundary circles are denoted by ∂A_1 and ∂A_2. It is evident

$$A = \{(x,y) |\, R_1^2 \leq x^2 + y^2 \leq R_2^2\}, \tag{4}$$

$$\partial A_i = \left\{(x,y) |\, x^2 + y^2 = R_i^2\right\} (i = 1,2). \tag{5}$$

The constitutive equations for orthotropic linearly piezoelectric material can be represented as

$$\gamma_{xz} = \vartheta\left(\frac{\partial\omega}{\partial x} - y\right) = f(r)[s_{55}\tau_{xz} + g_{15}D_x], \tag{6}$$

$$\gamma_{yz} = \vartheta\left(\frac{\partial\omega}{\partial y} + x\right) = f(r)\left[s_{44}\tau_{yz} + g_{24}D_y\right], \tag{7}$$

$$E_x = f(r)[-g_{15}\tau_{xz} + \beta_{11}D_x], \tag{8}$$

$$E_y = f(r)[-g_{24}\tau_{yz} + \beta_{22}D_y]. \tag{9}$$

In equations (6-9), $\omega = \omega(x,y)$ is the torsion function, γ_{xz} and γ_{yz} are the shearing strains, ϑ is the rate of twist, τ_{xz}, τ_{yz} are the shearing stresses D_x, D_y are the components of electric displacement vector and E_x, E_y are the components of the electric field vector, s_{55} and s_{44} are the shear flexibility coefficients, g_{15}, g_{24} are the piezoelectric constants, β_1, β_2 are the inverses of permittivity constants. The components of the electric field vectors are obtained from the electric potential field $\vartheta\phi$

$$E_x = -\vartheta\frac{\partial\phi}{\partial x}, \quad E_y = -\vartheta\frac{\partial\phi}{\partial y}. \tag{10}$$

According to the solutions of the stress equilibrium equation for τ_{xz} and τ_{yz} and Gauss equation for D_x and D_y they are expressed in terms of Prandt's stress function and electric displacement potential function [11,17] as

$$\tau_{xz} = \vartheta\frac{\partial U}{\partial y}, \quad \tau_{yz} = -\vartheta\frac{\partial U}{\partial x}, \tag{11}$$

$$D_x = \vartheta\frac{\partial F}{\partial y}, \quad D_y = -\vartheta\frac{\partial F}{\partial x}. \tag{12}$$

Here, $U = U(x,y)$ is the Prandtl's stress function and $F = F(x,y)$ is the electric displacement potential function. These functions satisfy the following boundary conditions [17]

$$U(x,y) = 0 \quad (x,y) \in \partial A_2,$$

$$U(x,y)=U_1=\text{const.}\quad (x,y)\in\partial A_1, \tag{13}$$

$$F(x,y)=0\quad (x,y)\in\partial A_2\,,$$
$$F(x,y)=F_1=\text{const.}\quad (x,y)\in\partial A_1. \tag{14}$$

3 Formulation of the solution

It is assumed that

$$\omega(x,y)=C_\omega xy\qquad \phi(x,y)=C_\phi xy, \tag{15}$$

$$\frac{\partial U}{\partial\varphi}=0\qquad \frac{\partial F}{\partial\varphi}=0, \tag{16}$$

that is $U=U(r)$, $F=F(r)$. In this case, from equations (6-9) and (10), (15) and (16) it follows that

$$C_\omega-1=\frac{f(r)}{r}\left[s_{55}\frac{\partial U}{\partial r}+g_{15}\frac{\partial F}{\partial r}\right], \tag{17}$$

$$C_\omega+1=-\frac{f(r)}{r}\left[s_{44}\frac{\partial U}{\partial r}+g_{25}\frac{\partial F}{\partial r}\right], \tag{18}$$

$$-C_\phi=\frac{f(r)}{r}\left[-g_{15}\frac{\partial U}{\partial r}+\beta_{11}\frac{\partial F}{\partial r}\right], \tag{19}$$

$$C_\phi=\frac{f(r)}{r}\left[g_{24}\frac{\partial U}{\partial r}-\beta_{22}\frac{\partial F}{\partial r}\right]. \tag{20}$$

Combination of equation (17) with equation (18) gives

$$s\frac{\partial U}{\partial r}+g\frac{\partial F}{\partial r}=-2\frac{r}{f(r)}\qquad R_1\le r\le R_2, \tag{21}$$

where

$$s=s_{55}+s_{44}\qquad g=g_{15}+g_{24}. \tag{22}$$

From equations (19) and (20) we obtain

$$g\frac{\partial U}{\partial r}-\beta\frac{\partial F}{\partial r}=0\qquad R_1\le r\le R_2, \tag{23}$$

$$\beta=\beta_{11}+\beta_{22}. \tag{24}$$

The solution of the system of equations (21) and (23) for $\frac{\partial U}{\partial r}$ and $\frac{\partial F}{\partial r}$ are

$$\frac{\partial U}{\partial r}=-\frac{-2\beta}{s\beta+g^2}\frac{r}{f(r)}\qquad R_1\le r\le R_2, \tag{25}$$

$$\frac{\partial F}{\partial r}=-\frac{2g}{s\beta+g^2}\frac{r}{f(r)}\qquad R_1\le r\le R_2. \tag{26}$$

From equations (25) and (26) under the boundary conditions

$$U(R_2)=0\qquad F(R_2)=0 \tag{27}$$

it follows that

$$U(r)=\frac{2\beta}{s\beta+g^2}\int_r^{R_2}\frac{\rho}{f(\rho)}\mathrm{d}\rho, \tag{28}$$

$$U(R_1)=\frac{2\beta}{s\beta+g^2}\int_{R_1}^{R_2}\frac{\rho}{f(\rho)}\mathrm{d}\rho, \tag{29}$$

$$F(r)=\frac{2g}{s\beta+g^2}\int_r^{R_2}\frac{\rho}{f(\rho)}\mathrm{d}\rho, \tag{30}$$

$$F(R_1)=\int_{R_1}^{R_2}\frac{\rho}{f(\rho)}\mathrm{d}\rho. \tag{31}$$

The expression of shearing stresses τ_{rz} and $\tau_{r\varphi}$ are

$$\tau_{rz}=0\qquad \tau_{\varphi z}=-\varphi\frac{\partial U}{\partial r}=\frac{2\phi r\beta}{(s\beta+g^2)f(r)}. \tag{32}$$

The radial and tangential components of the electric displacement vector are

$$D_r=0\qquad D_\varphi=-\vartheta\frac{\partial F}{\partial r}=\frac{2\vartheta rg}{(s\beta+g^2)f(r)}. \tag{33}$$

The expression of the elastic torsional rigidity S_E is obtained as

$$S_E=\frac{T}{\vartheta}=$$
$$=\frac{1}{\vartheta}\int_{R_1}^{R_2}2\pi r^2\tau_{\varphi z}\mathrm{d}r=\frac{4\pi\beta}{s\beta+g^2}\int_{R_1}^{R_2}\frac{r^3}{f(r)}\mathrm{d}r. \tag{34}$$

The electric torsional rigidity S_D is defined as

$$S_D=\frac{1}{\vartheta}\int_{R_1}^{R_2}2\pi r^2D_\varphi\mathrm{d}r=\frac{4\pi\beta}{s\beta+g^2}\int_{R_1}^{R_2}\frac{r^3}{f(r)}\mathrm{d}r. \tag{35}$$

It is evident

$$\frac{S_D}{S_E}=\frac{g}{\beta}. \tag{36}$$

The constant C_ω is obtained from equations (17) and (18). A simple computation gives

$$C_\omega=\frac{(s_{44}-s_{55})(\beta_{11}+\beta_{22})+g_{24}^2-g_{15}^2}{(s_{44}+s_{55})(\beta_{11}+\beta_{22})+(g_{15}+g_{24})^2}. \tag{37}$$

In a similar way the constant C_ϕ can be computed from equations (19) and (20)

$$C_\phi=\frac{(g_{24}-g_{15})(\beta_{11}+\beta_{22})+(g_{15}+g_{24})(\beta_{11}-\beta_{22})}{(s_{44}+s_{55})(\beta_{11}+\beta_{22})+(g_{15}+g_{24})^2}. \tag{38}$$

Equations (36) and (37) show that the torsion function $\omega(x,y)=C_\omega xy$ and electric potential function $\phi=C_\phi xy$ do not depend on the material inhomogeneity.

4 Elastic cylindrical body

For elastic cylindrical body

$$g_{15}=g_{24}=0. \tag{39}$$

In this case

$$U(r)=\frac{2}{s_{44}+s_{55}}\int_r^{R_2}\frac{\rho}{f(\rho)}\mathrm{d}\rho\qquad R_1\le r\le R_2, \tag{40}$$

$$F(r)=0\qquad R_1\le r\le R_2, \tag{41}$$

$$S_E = \frac{4\pi}{s_{44}+s_{55}} \int_{R_1}^{R_2} \frac{r^3}{f(r)} \mathrm{d}r \qquad S_D = 0, \tag{42}$$

$$C_\omega = \frac{s_{44}-s_{55}}{s_{44}+s_{55}} \qquad C_\phi = 0. \tag{43}$$

5 Numerical example

The following data are used in the numerical example:

$$R_1 = 0.01\ \mathrm{m}, R_2 = 0.02\ \mathrm{m}, \vartheta = 0.5 \times 10^{-2} \mathrm{rad/m}$$

$$f_1 = 0.2, f_2 = 0.8,$$

$$s_{55} = 1.927\,411\,813 \times 10^{-11}\ \mathrm{m^2/N}$$

$$s_{44} = 2.769\,957\,090 \times 10^{-11}\ \mathrm{m^2/N}$$

$$g_{15} = 0.038\,967\,890\,460\ \mathrm{m^2/C}$$

$$g_{24} = 0.047\,323\,389\,110\ \mathrm{m^2/C}$$

$$\beta_{11} = 7.673\,768\,900 \times 10^{7}\ \mathrm{Vm/C}$$

$$\beta_{22} = 4.676\,146\,855 \times 10^{7} \mathrm{Vm/C}$$

For power index $n = 1,2,3,4$ the graphs of $f(r,n)$ as a function of r are shown in Figure 2.

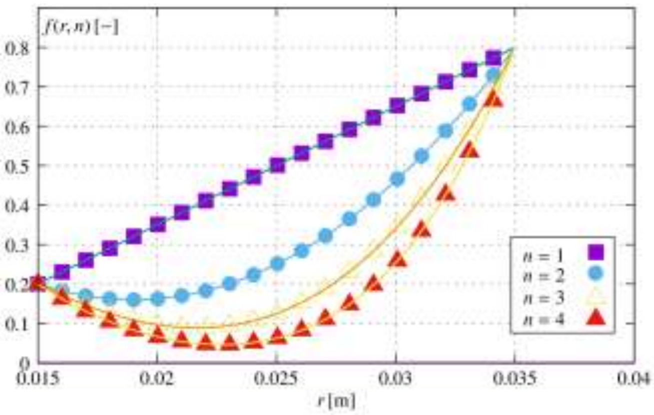

Fig. 2 *The plots of* $f(r,n)$ *as a function of* r.

The dependence of Prandtl's stress function from the power index n for $n = 1,2,3,4$ is presented in Figure 3.

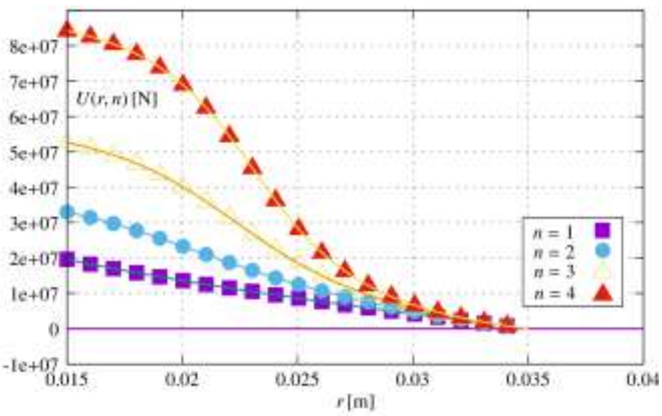

Fig. 3 *The graphs of the Prandtl's stress function for* $n = 1,2,3,4$ *as a function of* r.

The dependence of electric displacement function from the power index n for $n = 1,2,3,4$ is presented in Figure 4 as a function of radial coordinate r.

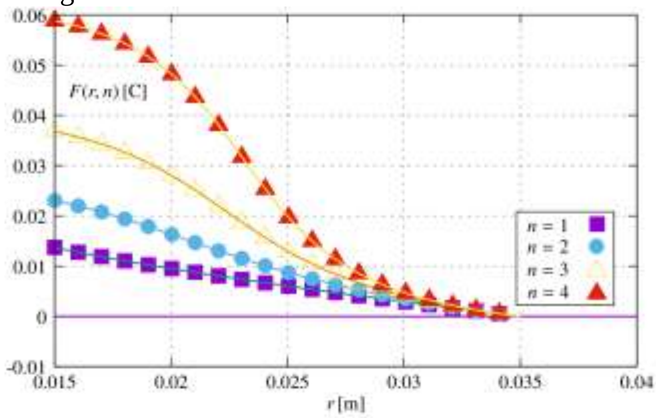

Fig. 4 *Plots of electric displacement function* $F(r,n)$ *for* $n = 1,2,3,4$ *and* $R_1 \leq r \leq R_2$.

Figure 5 and Figure 6 show the plots of shearing stress $\tau_{\varphi z}$ circular component of electric displacement vector for $n = 1,2,3,4$ as a function of radial coordinate r.

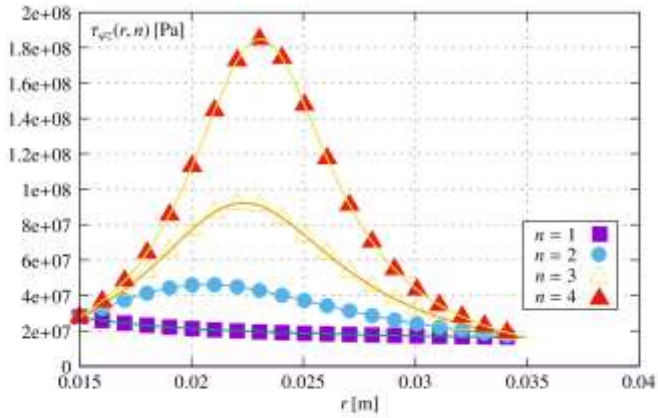

Fig. 5 *Plots of shearing stresses*.

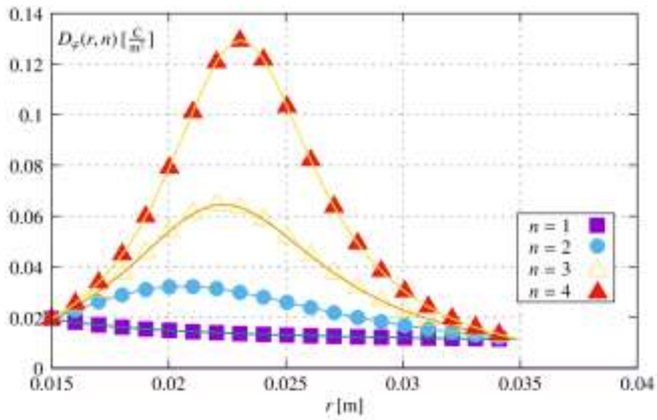

Fig. 6 *Plots of* $D_\varphi(r,n)$ *a function of* r *for* $n = 1,2,3,4$.

The elastic torsion rigidity S_E as a function of power index n is given in Figure 7 for $-6 \leq n \leq 6$.

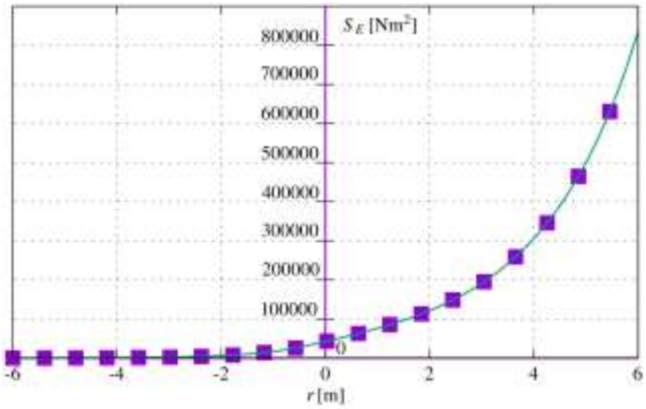

Fig. 7 *The torsional rigidity S_E as a function of n for* $-6 \leq n \leq 6$.

The dependence of electric torsional rigidity S_D from the power index n for $-6 \leq n \leq 6$ is shown in Figure 8.

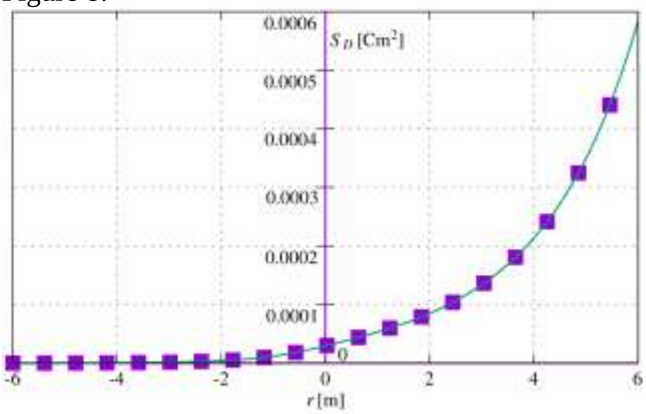

Fig. 8 *The electric torsional rigidity S_D as a function of n* $-6 \leq n \leq 6$.

5 Conclusion

An analytical solution is presented for the torsion of hollow and solid piezoelectric cylinder. The governing variables are the Prandtl's stress function and electric displacement potential function. The material of the cylinder is functional graded. It is a smooth power function of the radial coordinate. A complete solution is presented for the Saint-Venant torsion of orthotropic piezoelectric cylinder. The paper investigates the dependence of mechanical and electric fields from the power index of the radial inhomogeneity.

References:

[1] Altzoumalis, A.I., Kytopoulos, K.N.: A study of stress-induced suitable magnetic changes in mild steel unsing Barkhausen emission-aided analysis approaches, WSEAS Transactions on Electronics, vol. 14, pp. 24-33, 2023.

[2] Saleh, S., Elsimary, M., Zaki, A. Ahnad, S.: Design and fabrication of piezoelectric acoustic sensor. Proceedings of the 5th WSEAS Int. Conf. Microelectronics, Nanoelectronics, Optoelectronics, Prague, Czech Republic, March 12-14, 92—96, (2006).

[3] Lurie, A.I.: Theory of Elasticity. Fiz-Mat-Lit, Moscow (1970), In Russian.

[4] Sokolnikoff, I.S.: Mathematical Theory of Elasticity. McGraw-Hill, New York, (1956).

[5] Sadd, H.H.: Elasticity Theory: Applications and Numerics. Elsevier, London (2005).

[6] Lekhniskii, S.G.: Theory of Anisotropic and Non-Homogenous Beams. Nauka, Moscow (1971).

[7] Lekhniskii, S.G.: Theory of Elasticity of an Anisotropic Body. Mir Publishers, Moscow (1981), In Russian.

[8] Rooney, F.T.: Ferrai, M.: Torsion and Flexure of inhomogeneous elements Compos. Eng. 5(7), 901-911, (1995).

[9] Davi, F.: Saint-Venant's problem for linear piezoelectric bodies. Journ. Elasticity. 43, 227-245, (1996).

[10] Bisegna, P.: Saint-Venant problem in the linear problem of piezoelectricity. Atti Convegni LIncei. Accad. Naz. Licei Rome, 40, 151-165, (1998).

[11] Bisegna, P.: The Saint-Venant problem for monoclinic piezoelectric cylinders. ZAMM 78(3), 147-165, (1999).

[12] Horgan, C.O., Chan, A.M.: Torsion of functionally graded isotropic linearly elastic bars. Journ. Elasticity, 52(2), 181-189 (1999).

[13] Rovenski, V.E., Harash, E.: Abramovich, H.: Saint-Venant's problem for homogenous piezoelectric beams. TAE Report No.967, 1-100 (2000).

[14] Rovenski, V.E., Harash, E., Abramovich, H.: Saint-Venant's problem for

homogeneous piezoelectric beams, Journ. Appl. Mech. 47(6), 1095-1103 (2003).

[15] Rovenski, V.E., Abramovich, H.: Saint-Venant problem for compound piezoelectric beams. Journ. Elasticity, 96, 105-127 (2009).

[16] Horgan, C.O.: On the torsion of functionally graded anisotropic linearly elastic bars. IMA Journ. Appl. Math. 7(5), 556-562 (2007).

[17] Ecsedi, I., Baksa, A.: A Prandtl's formulation for the Saint-Venant's torsion of homogeneous piezoelectric beams. Int. Journ. Solids and Structures, 47, 3076-3083 (2010).

[18] Ecsedi, I., Baksa, A.: A variational formulation for the torsion problem of piezoelectric beams. Appl.Math.Model, 36, 1668-1677 (2012).

[19] Ecsedi, I., Baksa, A.: Torsion of functionally graded anisotropic linearly elastic circular cylinder. Eng. Transc. 66(4), 413-426, (2018).

[20] Ecsedi, I., Baksa, A.: Saint-Venant torsion of non-homogeneous orthotropic circular cylinder, Arch.Appl.Mech., 90, 815-827, (2020).

[21] Shen, H.S.: Functionally Graded Materials. Nonlinear Analysis of Plates and Shells. CRC Press, New York, (2009).

[22] Suresh, S.M.: Fundamentals of Functionally Graded Materials. IOM Communications Limited, London (1998).

Contribution of Individual Authors to the Creation of a Scientific Article (Ghostwriting Policy)

István Ecsedi and Attila Baksa carried out the investigation and the formal analysis. István Ecsedi has implemented the algorithm for all the examples. Attila Baksa was responsible for the validation and for the visualization of the results. Both authors have been writing the paper with original draft, review and editing.

Sources of Funding for Research Presented in a Scientific Article or Scientific Article Itself

The author(s) received no financial support for the research, authorship, and/or publication of this article. Furthermore, on behalf of all authors, the corresponding author states that there is no conflict of interest.

Conflicts of Interest

The authors have no conflicts of interest to declare that are relevant to the content of this article.